

DNA binding and cleavage activity of a structurally characterized Ni(II) Schiff base complex

SARAT CHANDRA KUMAR^a, ABHIJIT PAL^a, MERRY MITRA^a,
V M MANIKANDAMATHAVAN^b, CHIA -HER LIN^c, BALACHANDRAN UNNI NAIR^{b,*}
and RAJARSHI GHOSH^{a,*}

^aDepartment of Chemistry, The University of Burdwan, Burdwan 713 104, India

^bChemical Laboratory, Central Leather Research Institute, Adyar, Chennai 600 020, India

^cDepartment of Chemistry, Chung Yuan Christian University, Chung Li, Taiwan 32023, ROC

e-mail: rajarshi_chem@yahoo.co.in; bunair@clri.res.in

MS received 26 December 2014; revised 16 April 2015; accepted 27 April 2015

Abstract. Synthesis and characterization of a mononuclear Ni(II) compound [Ni(L)(H₂O)₂](NO₃)₂ [L = N,N'-bis((pyridine-2-yl)phenylidene)-1,3-diaminopropan-2-ol] (**1**) is reported. **1** crystallizes in triclinic P-1 space group with a = 8.1911(2) Å, b = 11.6624(3) Å, c = 16.5356(4) Å and α = 108.8120(10)°, β = 91.2010(10)°, γ = 91.1500(10)°. The binding property of the complex with DNA has been investigated using absorption and emission studies, and viscosity experiment. The binding constant (K_b) and the linear Stern-Volmer quenching constant (K_{sv}) of the complex have been determined as 9.23 × 10⁴ M⁻¹ and 2.0 × 10⁴ M⁻¹, respectively. Spectroscopic and hydrodynamic investigations revealed groove or electrostatic nature of binding of **1** with DNA. **1** is also found to induce oxidative cleavage of the supercoiled pUC 18 DNA to its nicked circular form in a concentration dependent manner.

Keywords. Nickel(II); Schiff base; crystal structure; DNA cleavage

1. Introduction

DNA is the primary intracellular target of an anticancer agent as the interaction between these biologically active molecules and DNA can cause the nucleic acid damage as well as blocking of division of cancer cells. The synthetic small molecules can bind to DNA in different modes like intercalation, groove binding, electrostatic interaction and mixed mode of binding. Nucleic acid cleavage by the naturally occurring enzyme nuclease is an important biochemical reaction leading to programmed cell death. Such cleavage often produces insights into the mechanism of action for antitumour antibiotics.^{1,2} Transition metal complexes have been exploited as probes for nucleic acid structure and showing nuclease activity.^{3,4} Schiff bases are important class of ligands in bioinorganic chemistry as its complexes show different biological activity including nucleic acid cleavage.^{3a,3b,5} A number of nickel complexes with nuclease activity are found in literature.⁶ In continuation of our recent interest in DNA cleavage activity³ of first row transition metal complexes we present here the synthesis, X-ray structure, and DNA binding

and cleavage activity of an octahedral Ni(II) complex [Ni(L)(H₂O)₂](NO₃)₂ [L = N,N'-bis((pyridine-2-yl)phenylidene)-1,3-diaminopropan-2-ol] (**1**).

2. Experimental

2.1 Materials

High purity 2-benzoylpyridine (Lancaster, UK), 1,3-diaminopropan-2-ol (Aldrich, UK), nickel(II) nitrate hexahydrate (E. Merck, India), Calf thymus DNA (CT DNA; Bangalore Genie, India), supercoiled pUC18 DNA (Cesium chloride purified, Bangalore Genie, India), agarose (molecular biology grade; Sigma, UK) and ethidium bromide (EB; Sigma, UK) were purchased from respective concerns and used as received.

2-benzoylpyridine (0.366 g, 2 mmol) was refluxed with 1,3-diaminopropan-2-ol (0.086 g, 1 mmol) in dehydrated alcohol. After 10 h, the solution was evaporated under reduced pressure to yield a gummy mass, which was dried and stored *in vacuo* over CaCl₂ for subsequent use. Yield, 0.291 g (70%). The ligand was purified chromatographically. Anal. cal. for C₂₇H₂₃N₄O: C, 77.30; H, 5.53; N, 13.36; Found: C, 76.52; H, 4.90; N, 12.92. IR (KBr pellet): 1632 (s), 3375 (s). ¹H NMR

*For correspondence

δ (ppm): 8.71 (d, $J = 4.0$ Hz, 1H), 8.06 (d, $J = 8$ Hz, 2H) (figure S1, Supplementary Information).

Solutions of CT DNA in 50 mM Tris-HCl (pH = 7.2) gave a ratio of UV absorbance at 260 and 280 nm, A_{260}/A_{280} of *ca.* 1.8-1.9, indicating that the DNA was sufficiently free of protein contamination. The DNA concentration was determined by the UV absorbance at 260 nm using molar absorption coefficient $6600 \text{ M}^{-1}\text{cm}^{-1}$. Stock solutions were kept at 4°C and used within 4 days.

2.2 Physical measurements

Elemental analyses (C, H, N) were performed on a Perkin-Elmer 2400 CHNS/O elemental analyzer. IR spectra (KBr discs, $4000\text{--}300 \text{ cm}^{-1}$) were recorded using a Perkin-Elmer FT-IR model RX1 spectrometer. Thermal analysis was done on PerkinElmer Diamond TG/DTA system. Absorption and steady-state fluorescence measurements were made with a Jasco model V-530 UV-Vis spectrophotometer and Hitachi model F-4010 spectrofluorimeter, respectively.

Viscosity measurements were carried out using an Oswald-type viscometer, thermostated in a water bath maintained at $25 (\pm 0.1)^\circ\text{C}$. The viscosity for DNA ($100 \mu\text{M}$) was measured in the presence and absence of the complex ($0\text{--}80 \mu\text{M}$). Flow time was measured with a digital stopwatch and the average of triplicate of the experiment was used. The relative viscosities for DNA in the absence (η_0) and presence (η) of the complex was calculated using the relation $\eta = (t-t_0)/t_0$, where t and t_0 are the observed flow time for sample and buffer. The values of relative viscosity $(\eta/\eta_0)^{1/3}$ were plotted against $R = [\text{complex}]/[\text{DNA}]$.

The cleavage of plasmid DNA was monitored using agarose gel electrophoresis. Super coiled pUC18 DNA (200 ng) in Tris buffer (10 mM , pH 7.2) with 50 mM NaCl was treated with the complex ($0\text{--}60 \mu\text{M}$). The samples were incubated for 30 min in the presence of additive H_2O_2 ($100 \mu\text{M}$). A loading buffer containing 0.25% bromophenol blue, 40% (w/v) sucrose and 0.5 MEDTA was added and the electrophoresis of the DNA cleavage product was performed on 0.8% agarose gel containing $0.5 \mu\text{g/mL}$ ethidium bromide (EB). The gel was run at 50 V for 2 h in Tris-boric acid-EDTA (TBE) buffer and the bands were photographed by a UV-Chemi Gel documentation system.

2.3 Preparation of **1**

Mononuclear complex **1** was prepared from nitrate salt of nickel(II) using 1:1 mole ratio of the metal

and L [L = N,N'-bis((pyridine-2-yl)phenylidene)-1,3-diaminopropan-2-ol]. Typical synthesis is described below:

A methanolic solution (5 mL) of L (0.416 g , 1 mmol) was added dropwise to a solution of $\text{Ni}(\text{NO}_3)_2 \cdot 6\text{H}_2\text{O}$ (0.290 g , 1 mmol) in the same solvent (10 mL). The light green solution was filtered and the supernatant liquid was kept in air for slow evaporation. After a few days, the complex **1** that separated out was washed in hexane and dried *in vacuo* over silica gel indicator. Yield, 0.267 g (40%). Anal. cal. for $\text{C}_{27}\text{H}_{27}\text{N}_6\text{O}_9\text{Ni}$ (**1**): C, 50.85; H, 4.27; N, 13.18; Found: C, 50.10; H, 4.40; N, 12.10. IR (KBr pellet): 1380 (m) , 1593 (m) , 1630 (m) , 3377 (s) .

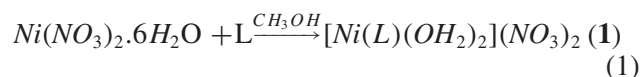
2.4 X-ray diffraction study

Single crystals of **1** for X-ray crystallographic analysis were selected following examination under a microscope. Diffraction data at $295(2) \text{ K}$ were collected on a Bruker SMART APEX II CCD diffractometer using Mo- $\text{K}\alpha$ radiation ($\lambda = 0.71073 \text{ \AA}$). The crystal data and refinement details are listed in table 1. **1** was identified as *P-1* space group. The structure was solved by direct methods, and the structure solution and refinement were based on $|F|^2$. The final differences All calculations were carried out using SHELXL-97.⁷ All the figures have been generated using ORTEP-32.⁸

3. Results and Discussion

3.1 Synthesis and formulation

The ligand L [N,N'-bis((pyridine-2-yl)phenylidene)-1,3-diaminopropan-2-ol] (scheme 1) was synthesized by refluxing 1,3-diaminopropan-2-ol and 2-benzoylpyridine in 1:2 molar ratio in boiling alcohol. Light green coloured crystalline hexacoordinated mononuclear complex $[\text{Ni}(\text{L})(\text{OH}_2)_2](\text{NO}_3)_2$ (scheme 1) (**1**) resulted in good yield through single pot reaction of 1:1 molar ratio of the nickel(II) nitrate hexahydrate and ligand in methanolic solution. The synthetic procedure is summarized in scheme 1.



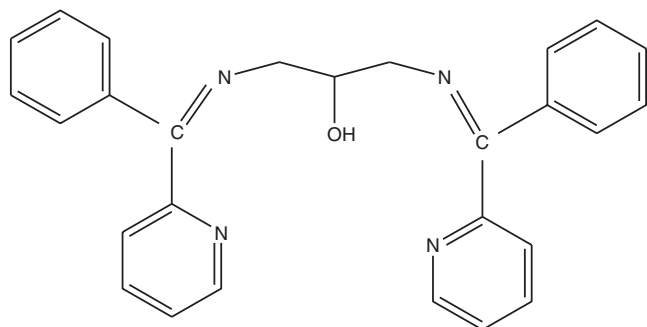
The complex is sufficiently stable in air and in presence of moisture. Analytical data for all the complexes are consistent with the calculated values. The compound is soluble in dimethyl formamide (DMF). In IR spectrum of **1**, the most striking observation is a sharp and intense band due to nitrate⁹ at 1380 cm^{-1} . The $\nu(\text{C}=\text{N})$ stretching vibrations of the metal bound Schiff base are seen at 1593 and 1630 cm^{-1} . All other characteristic ligand vibrations are seen in $1600\text{--}600 \text{ cm}^{-1}$.

Table 1. Crystal data and structure refinement parameters for **1**.

Empirical formula	C ₂₇ H ₂₇ N ₆ O ₉ Ni
Formula weight	638.26
T (K)	295(2) K
Wavelength (Å)	0.71073 Å
Crystal system	Triclinic
Space group	P-1
Unit cell dimensions	
a (Å)	8.1911(2) Å
b (Å)	11.6624(3) Å
c (Å)	16.5356(4) Å
α (°)	108.8120(10)°
β (°)	91.2010(10)°
γ (°)	91.1500(10)°
V (Å ³)	1494.30(6) Å ³
Z	2
D _{calc} (mg/m ³)	1.419 Mg/m ³
Absorption coefficient (mm ⁻¹)	0.710 mm ⁻¹
F(000)	662
Crystal size (mm ³)	0.25 × 0.25 × 0.15 mm ³
Theta range for data collection (°)	1.85 to 28.29°
Index ranges	-10 ≤ h ≤ 10, -15 ≤ k ≤ 15, -22 ≤ l ≤ 21
Reflections collected	27691
Independent reflections	7409 [R(int) = 0.0766]
Completeness to theta	99.8 %
Absorption correction	Semi-empirical from equivalents
T _{max} and T _{min}	0.901 and 0.812
Refinement method	Full-matrix least-squares on F ²
Data/restraints/parameters	7409/ 5/390
Goodness-of-fit (GOF) on F ²	1.099
Final R indices [I > 2σ(I)]	R1 = 0.0679, wR2 = 0.2222
R indices (all data)	R1 = 0.0846, wR2 = 0.2336
Largest difference in peak and hole (eÅ ⁻³)	1.346 and -1.056 e.Å ⁻³
wR2 = [∑w(F _o ² - F _c ² ²)/ ∑w(F _o ² ²)] ^{1/2} , w = [σ ² (F _o ²) + 0.1427P] ² + 0.3463P], (where P = (F _o ² + 2F _c ²)/3)	

3.2 X-ray structure

An Oak Ridge Thermal Ellipsoid Plot (ORTEP) with atom numbering scheme of the mononuclear complex **1** is shown in (figure 1). Selected bond angles and



L

Scheme 1. Ligand structure and preparation of **1**.

bond lengths relevant to the coordination sphere are listed in (table 2). The crystal lattice of **1** consists of [Ni(L)(OH₂)₂]²⁺ cations and order and highly disorder NO₃⁻ anions. The coordination polyhedron around each Ni(II) is best described as distorted octahedron with

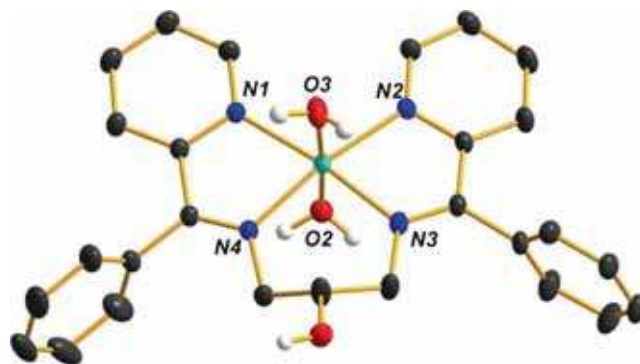
**Figure 1.** An ORTEP of [Ni(L)(H₂O)₂](NO₃)₂ (**1**) with atom numbering scheme and 20% probability ellipsoids for all non-hydrogen atoms.

Table 2. Bond lengths [Å] and angles [°] for **1**.

Bond distances			
Ni(1)-N(4)	2.049(2)	Ni(1)-N(2)	2.092(3)
Ni(1)-N(3)	2.063(3)	Ni(1)-O(2)	2.093(2)
Ni(1)-O(3)	2.086(3)	Ni(1)-N(1)	2.104(3)
Bond angles			
N(4)-Ni(1)-N(3)	93.80(10)	O(3)-Ni(1)-O(2)	175.89(10)
N(4)-Ni(1)-O(3)	93.59(11)	N(2)-Ni(1)-O(2)	89.94(10)
N(3)-Ni(1)-O(3)	91.17(11)	N(4)-Ni(1)-N(1)	78.96(10)
N(4)-Ni(1)-N(2)	171.24(10)	N(3)-Ni(1)-N(1)	172.75(10)
N(3)-Ni(1)-N(2)	78.60(10)	O(3)-Ni(1)-N(1)	89.19(11)
O(3)-Ni(1)-N(2)	90.93(11)	N(2)-Ni(1)-N(1)	108.64(10)
N(4)-Ni(1)-O(2)	86.09(10)	O(2)-Ni(1)-N(1)	86.72(10)
N(3)-Ni(1)-O(2)	92.94(11)	O(3)-Ni(1)-O(2)	175.89(10)

a NiN₄O₂ chromophore. The distortion from the ideal octahedral geometry is due to the asymmetric nature of the bound tetradentate Schiff base and the deviations of the refine angles formed at the metal centre (table 2). The metal ion is ligated by two pyridine nitrogens (N1 and N2), two imine nitrogens (N3 and N4) and two oxygen atoms of coordinated water molecules (O2 and O3) in *cis-cis-trans* orientation. The two pyridine nitrogens (N1 and N2) and two imine nitrogens (N3 and N4) occupy the equatorial positions of the distorted octahedron, whereas the axial positions are occupied by two water oxygen atoms (O2 and O3). The Ni-N/O bond distances range from 2.049(2)-2.104(3) Å and the difference between the longest and shortest Ni-N/O bonds amounts 0.055 Å. The residual electron density with largest diff. peak with 1.346 eÅ⁻³ might be caused by the disorder of nitrate anions.

3.3 Studies on interaction of **1** with DNA and DNA cleavage

3.3a UV-Vis spectroscopy: The DNA binding experiments were performed in Tris-HCl buffer (50 mM Tris-HCl, pH 8) using a tris base solution of the complex **1**. The concentration of DNA was determined from the absorbance at 260 nm with an ϵ value¹⁰ of 6600 M⁻¹cm⁻¹. Absorption titration experiments were made using different concentrations of CT-DNA, while keeping the complex concentration constant. Due correction was made for the absorbance of the DNA itself. Samples were equilibrated before recording each spectrum. A broad spectrum in the range 250-280 nm is shown in the UV-Vis spectrum of the complex (figure 2). After addition of DNA to the solution of Ni(II) complex in tris-buffer, it is clearly observed that the absorption peak at 270 nm undergoes a significant decrease in molecular absorption (hypochromic effect) with no

detectable shift in the absorption wave length. The gradual decrease in the absorption wavelength indicates some interaction of **1** with DNA double strand. The binding constant, K_b for the complex has been determined⁵ from the plot of [DNA]/($\epsilon_A - \epsilon_F$) vs. [DNA] and found to be $K_b = 9.23 \times 10^4 \text{M}^{-1}$ ($R = 0.99732$ for four points) (figure 2, inset).

3.3b Fluorescence spectroscopy: The fluorescence spectral method using the standard intercalator ethidium bromide (EB) as a reference was used to determine the relative DNA binding properties of the complex **1** to the DNA in tris-buffer (5 mM, pH 8.0). Fluorescence intensities of EB in DNA were measured at different complex concentrations. The addition of the complex to the DNA pretreated with EB causes an appreciable reduction in the fluorescence intensity (figure 3) indicating that **1** competes with EB to bind with DNA. The reduction of the emission intensity gives a measure of the DNA binding propensity of the complex and stacking interaction (intercalation) between adjacent DNA base pairs.¹¹ The relative binding tendency of the complex with the DNA was determined by the comparison of the slope of the lines in the fluorescence intensity versus [complex] plot.

The quenching of EB bound to DNA by the complex **1** is in agreement with the linear Stern-Volmer equation:

$$I_0/I = 1 + K_{sv} [\text{complex}] \dots \quad (2)$$

where I_0 and I represent the fluorescence intensities in the absence and presence of quencher, respectively. K_{sv} is the linear Stern-Volmer quenching constant. From the slope of the regression line in the plot of I/I_0 versus [complex] (figure 3, inset), the K_{sv} value for the complex was found to be $9.23 \times 10^4 \text{M}^{-1}$ ($R = 0.99732$ for four points) indicating a strong affinity of the complex to DNA.

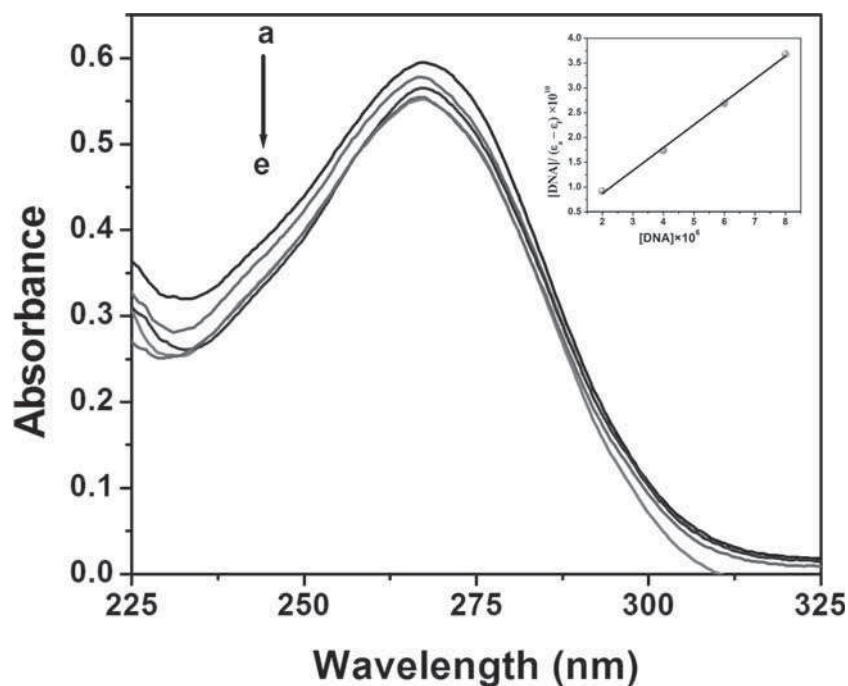


Figure 2. Electronic spectra of the title complex through titration with CT-DNA in Tris-HCl buffer; [Complex] = 1.02×10^{-4} M; [DNA]: (a) 0.0, (b) 2.0×10^{-6} , (c) 4.0×10^{-6} , (d) 6.0×10^{-6} , (e) 8.0×10^{-6} mol L $^{-1}$. The increase of DNA concentration is indicated by an arrow. [inset: Plot of $[DNA]/(\epsilon_A - \epsilon_F)$ vs. $[DNA]$ for the titration of CT-DNA with **1** in tris-HCl buffer, binding constant $K_b = 9.23 \times 10^4$ M $^{-1}$ ($R = 0.99732$)].

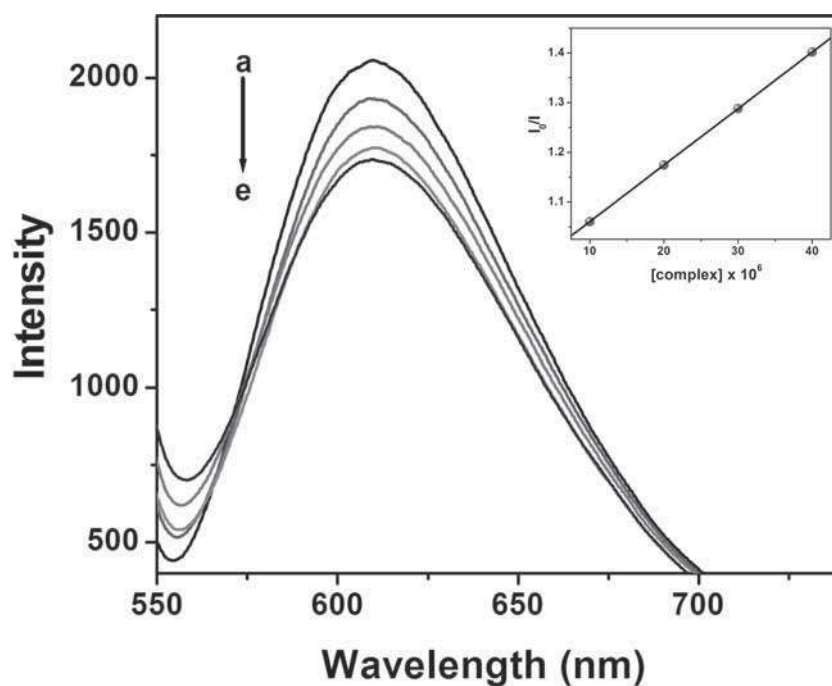


Figure 3. Fluorescence spectra of the CT-DNA-EB system in tris-HCl buffer based on the titration of **1**. $k_{ex} = 522$ nm; The arrow indicates the decrease of the complex concentration [inset: Plot of I/I_0 vs. $[complex]$ for the titration of CT-DNA-EB system with **1**; linear Stern-Volmer quenching constant $K_{sv} = 2.0 \times 10^4$ M $^{-1}$ ($R = 0.998$)].

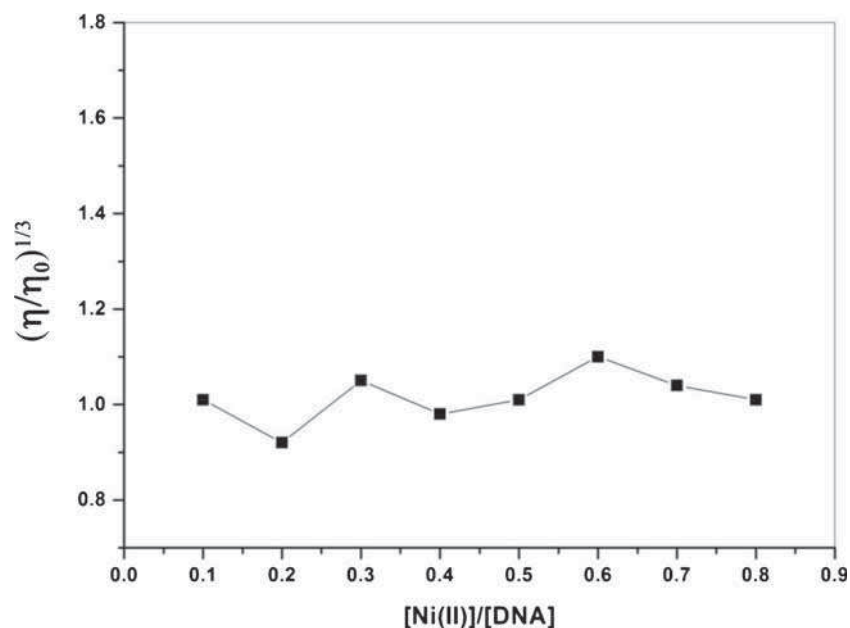


Figure 4. Effect of increasing amount of **1** (0–80 μM) on the relative viscosity of CT DNA (100 μM) at 25 (± 0.1) $^\circ\text{C}$.

3.3c Hydrodynamic studies: To further probe and distinguish between a groove binding, intercalative or partial intercalative and groove binding modes, viscosity of the DNA solution was measured in the presence of increasing concentration of **1** and the change in relative viscosities were estimated.¹² Hydrodynamic method provides unequivocal evidence for the mode of binding.^{13,14} The effect of addition of an increasing concentration of the complex on the relative viscosity of DNA is shown in figure 4. Classical intercalator groove and electrostatic binder show no change in viscosity.^{14a,15} Figure 4 shows that relative viscosity of DNA shows no change in the viscosity with increase in concentration of complex. This clearly shows groove or electrostatic binding nature of **1**.

3.3d Gelectrophoresis: DNA cleaving ability of the Ni(II) complex **1** has been studied using agarose

gel electrophoresis technique. The cleavage experiment was performed on pUC18 plasmid DNA. Incubation (6 h) of the complex (0–100 μM) with DNA did not result in any DNA cleavage. However, the complex when incubated with DNA in the presence of H_2O_2 brought about DNA cleavage as can be seen from Lanes 1 and 2 in figure 5, which are control DNA and DNA + H_2O_2 , which show the presence of supercoiled DNA (Form I) and a small amount of nicked DNA (Form II). In the presence of 10, 30 and 60 μM of the Ni(II) complex and 100 μM of H_2O_2 , supercoiled DNA is converted to nicked form of DNA in a concentration dependent manner. In order to check the mode of DNA cleavage mechanism different additives such as sodium azide, dimethylsulphoxide (DMSO) and heavy water (D_2O) have been used. As can be seen from the lanes 6 and 8, nicking of DNA brought about by Ni(II) complex is not prevented by sodium azide or enhanced by D_2O . This clearly indicates that singlet oxygen is not responsible

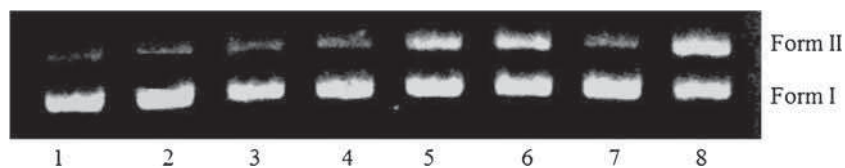


Figure 5. Lane 1: control pUC18 DNA [(200 ng) in Tris buffer (10 mM, pH 7.2) with 50 mM NaCl]; Lane 2: DNA + H_2O_2 + Control; Lane 3: DNA + **1** (10 μM) + H_2O_2 ; Lane 4: DNA + **1** (30 μM) + H_2O_2 ; Lane 5: DNA + **1** (60 μM) + H_2O_2 ; Lane 6: DNA + **1** (60 μM) + H_2O_2 + NaN_3 (100 μM); Lane 7: DNA + **1** (60 μM) + H_2O_2 + DMSO (3 μL); Lane 8: DNA + **1** (60 μM) + H_2O_2 + D_2O (3 μL).

for the DNA cleavage by Ni(II) complex. In the presence of DMSO (lane 7) nicking of DNA brought about by the Ni(II) complex in the presence of H₂O₂ is inhibited. This clearly indicates that hydroxyl radical is the responsible species for the observed cleavage of DNA.

4. Conclusion

In the present investigation, we have reported synthesis, single crystal X-ray structural characterization of a nickel(II) complex (**1**) with the Schiff base ligand L. Here, interaction of **1** with DNA has been studied. The binding constant for the complex is found to be $9.23 \times 10^4 \text{ M}^{-1}$ ($R = 0.99732$ for four points) which is similar to the reported values.^{3c,6b,15b} The linear Stern-Volmer quenching constant was determined as $2.0 \times 10^4 \text{ M}^{-1}$ ($R = 0.998$ for four points). Spectroscopic and hydrodynamic measurements provided evidence for groove or electrostatic nature of binding of **1** into the DNA double helix. **1** also induces concentration dependent oxidative cleavage of the supercoiled DNA. The hydroxyl radical of the hydrogen peroxide is responsible for the cleavage.

Supplementary Information

CCDC 1027532 contains the supplementary crystallographic data for **1**. These data can be obtained free of charge via <http://www.ccdc.cam.ac.uk/conts/retrieving.html>, or from the Cambridge Crystallographic Data Centre, 12 Union Road, Cambridge CB2 1EZ, UK; fax: (+44) 1223-336-033; or e-mail: deposit@ccdc.cam.ac.uk. NMR spectrum of L is also available with the supplementary information (figure S1). Supplementary Information is available at www.ias.ac.in/chemsci.

Acknowledgements

Financial support by the Department of Science & Technology, Government of West Bengal, India [No. 781(Sanc.)/ST/P/S&T/4G-4/2013 dated 04-12-2014] is gratefully acknowledged by RG. MM is thankful to The University of Burdwan for her fellowship.

References

- (a) Basu U, Khan I, Hussain A, Kondaiah P and Chakravarty A R 2012 *Angew. Chem. Int. Ed.* **51** 2658; (b) Basu U, Khan I, Koley D, Saha S, Kondaiah P and Chakravarty A R 2012 *J. Inorg. Biochem.* **116** 77; (c) Rajalakshmi S, Weyhermüller T, Dinesh M and Nair B U 2012 *J. Inorg. Biochem.* **117** 48; (d) Rajalakshmi S, Kiran M S and Nair B U 2014 *Eur. J. Med. Chem.* **80** 393
- (a) Walker M G, Gonzalez V, Chekmeneva E and Thomas J A 2012 *Angew. Chem. Int. Ed.* **51** 12107; (b) Fabbro C, Ali-Boucetta H, Ros T D, Kostarelos K, Bianco A and Prato M 2012 *Chem. Commun.* **48** 3911; (c) Farrer N J, Salassa L and Sadler P J 2009 *Dalton Trans.* 10690
- (a) Pal A, Biswas B, Mitra M, Rajalakshmi S, Purohit C S, Hazra S, Kumar S G, Nair B U and Ghosh R 2013 *J. Chem. Sci.* **125** 1161; (b) Biswas B, Mitra M, Pal A, Basu A, Rajalakshmi S, Mitra P, Aliaga-Alcalde N, Kumar G S, Nair B U and Ghosh R 2013 *Indian J. Chem.* **52A** 1576; (c) Mal S K, Mitra M, Kaur G, Manikandamadhavan V M, Kiran M S, Roy Choudhury A, Nair B U and Ghosh R 2014 *RSC Adv.* **4** 61337
- (a) Anbu S and Kandaswami M 2011 *Polyhedron* **30** 123; (b) Li D - D, Tian J - L, Gu W, Liu X, Zeng H - H and Yan S - P 2011 *J. Inorg. Biochem.* **105** 894; (c) Jaividhya P, Dhivya R, Akbarsha M A and Palaniandavar M 2012 *J. Inorg. Biochem.* **114** 94
- (a) Chaviara A T, Kioseoglou E E, Pantazaki A A, Tsipis A C, Karipidis P A, Kyriakidis D A and Bolos C A 2008 *J. Inorg. Biochem.* **102** 1749; (b) Chaviara A T, Cox P J, Repana K H, Pentazaki A A, Papazisis K T, Kortsaris A H, Kyriakidis D A, Nikolov G S and Bolos C A 2005 *J. Inorg. Biochem.* **99** 467; (c) Vijayalakshmi R, Kanthimati M, Subhramanian V and Nair B U 2000 *Biochim. Biophys. Acta* **1475** 157
- (a) Kasuga N C, Sekino K, Koumo C, Shimada N, Ishikawa M and Nomiyama K 2001 *J. Inorg. Biochem.* **84** 55; (b) Shahabadi N and Fatahi A 2010 *J. Mol. Struct.* **970** 90; (c) Skyrianou K C, Efthimiadou E K, Psycharis V, Terzis A, Kessissoglou D P and Psomas G 2009 *J. Inorg. Biochem.* **103** 1617; (d) Reed J E, Arnal A A, Neidle S and Vilar R 2006 *J. Am. Chem. Soc.* **128** 5992
- SHELXTL 5.10 (1997) Bruker Analytical X-ray Instruments Inc., Karlsruhe, Germany
- Farrugia L J, 1998, ORTEP-32 for Windows. University of Glasgow, Scotland.
- (a) Nakamoto K 1997 In *Infrared and Raman Spectra of Inorganic and Coordination Compounds, part B: Applications in Coordination, Organometallic, and Bioinorganic Chemistry* (New York: John Wiley); (b) Barbara S 2004 In *Infrared Spectroscopy: Fundamentals and Applications* (New York: Wiley)
- Reichmann M E, Rice S A, Thomas C A and Doty P 1954 *J. Am. Chem. Soc.* **76** 3047
- Lepecq J B and Paoletti C 1967 *J. Mol. Biol.* **27** 87
- Sinha R, Islam M M, Bhadra K, Kumar G S, Banerjee A and Maiti M 2006 *Bioorg. Med. Chem.* **14** 800
- Satyanarayana S, Dabrowiak J C and Chaires J B 1953 *Biochemistry* **32** 2573
- (a) Sasmal P K, Patra A K, Nethaji M and Chakravarty A R 2007 *Inorg. Chem.* **46** 11112; (b) Mahadevan S and Palaniandavar M 1998 *Inorg. Chem.* **37** 693; (c) Yang X -B, Huang Y, Zhang J -S, Yuan S -K and Zeng R -Q 2010 *Inorg. Chem. Commun.* **13** 1421
- (a) Roy S, Patra A K, Dhar S and Chakravarty A R 2008 *Inorg. Chem.* **47** 5625; (b) Roy M, Santhanagopal S and Chakravarty A R 2009 *Dalton Trans.* 1024